

Photo-induced surface frustrated Lewis pairs for promoted photocatalytic decomposition of perfluorooctanoic acid

Xianjun Tan, Zhenying Jiang, Yuxiong Huang (✉)

Tsinghua-Berkeley Shenzhen Institute (TBSI), Shenzhen International Graduate School, Tsinghua University, Shenzhen 518055, China

HIGHLIGHTS

- Terminal carboxylate group activation is PFOA degradation's rate-limiting step.
- $\text{Bi}_3\text{O}(\text{OH})(\text{PO}_4)_2$ with surface frustrated Lewis pairs (SFLPs) efficiently degrade PFOA.
- Photo-induced Lewis acidic sites and proximal surface hydroxyls constitute SFLPs.
- SFLPs act as collection centers to effectively adsorb PFOA.
- SFLPs endow accessible pathways for photogenerated holes rapid transfer to PFOA.

ARTICLE INFO

Article history:

Received 19 February 2022

Revised 29 June 2022

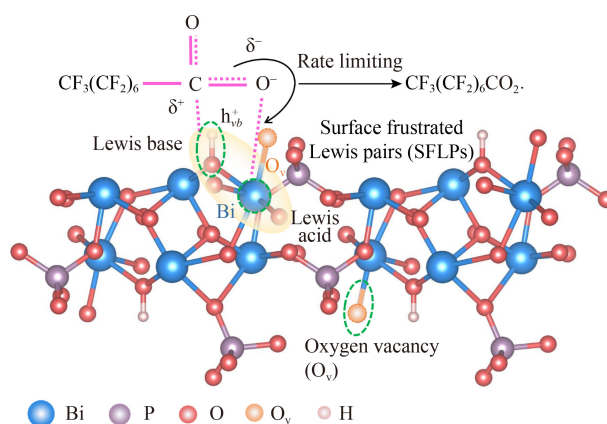
Accepted 29 June 2022

Available online 3 August 2022

Keywords:

Heterogeneous photocatalysis
Surface frustrated Lewis pairs
Perfluorooctanoic acid
Defluorination efficiency
Environmental remediation

GRAPHIC ABSTRACT



ABSTRACT

Heterogeneous photocatalysis has gained substantial research interest in treating per- and polyfluoroalkyl substances (PFAS)-contaminated water. However, sluggish degradation kinetics and low defluorination efficiency compromise their practical applications. Here, we report a superior photocatalyst, defected $\text{Bi}_3\text{O}(\text{OH})(\text{PO}_4)_2$, which could effectively degrade typical PFAS, perfluorooctanoic acid (PFOA), with high defluorination efficiency. The UV light irradiation could *in situ* generate oxygen vacancies on $\text{Bi}_3\text{O}(\text{OH})(\text{PO}_4)_2$ through oxidation of the lattice hydroxyls, which further promotes the formation of Lewis acidic coordinately unsaturated bismuth sites. Then, the Lewis acidic sites couple with the proximal surface hydroxyls to constitute the surface frustrated Lewis pairs (SFLPs). With the in-depth spectroscopic analysis, we revealed that the photo-induced SFLPs act as collection centers to effectively adsorb PFOA and endow accessible pathways to transfer photogenerated holes to PFOA rapidly. Consequently, activation of the terminal carboxyl, a rate-limiting step for PFOA decomposition, could be easily achieved over the defected $\text{Bi}_3\text{O}(\text{OH})(\text{PO}_4)_2$ photocatalyst. These results suggest that SFLPs exhibit great potential in developing highly efficient photocatalysts to degrade persistent organic pollutants.

© Higher Education Press 2023

Per- and polyfluoroalkyl substances (PFAS), a class of thousands of synthetic chemicals with perfluorinated carbon moieties, have attracted ever-increasing attention due to their physical stability, chemical resistance and extreme environmental persistence (Cordner et al., 2021; Ng et al., 2021; Qian et al., 2021; Qiao et al., 2021). As one of the most prevalent PFAS, perfluorooctanoic acid

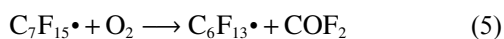
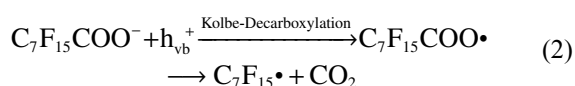
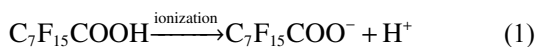
(PFOA) has been widely incorporated into consumer products, and released into various environmental media during the life cycle (Mumtaz et al., 2019; Garnett et al., 2021; Zheng et al., 2021). PFOA is persistent, which can exert multiple adverse effects on ecosystems and human health. Despite the rising concerns on the environmental risks, the development of effective technologies for PFOA decontamination remains in its infancy (Lu et al., 2020; Yang, 2020).

Recently, research interest has been directed to

✉ Corresponding author

E-mail: huang_yuxiong@sz.tsinghua.edu.cn

heterogeneous photocatalysis due to its capability of effectively destructing PFOA, but it suffers from sluggish degradation kinetics and low defluorination efficiency (Liu et al., 2020; Sun et al., 2020; Tan et al., 2020; Ding et al., 2021). For example, Zhang et al. reported the effective photocatalytic degradation of PFOA by nanostructured In_2O_3 , but it requires a long degradation period to obtain a limited defluorination efficiency (33.7%) (Li et al., 2012). Generally, the primary pathways for the photocatalytic oxidation of PFOA involve the following steps (Eqs. (1)–(6)) (Sun et al., 2020):



It is noteworthy that the Kolbe-Decarboxylation reaction requires high-energy consumption, which is considered to be the rate-limiting step for photocatalytic oxidation of PFOA (Sun et al., 2020). The intermediates such as $\text{C}_7\text{F}_{15}\cdot$, $\text{C}_7\text{F}_{15}\text{OH}$, $\text{C}_6\text{F}_{13}\text{COF}$ and COF_2 are unstable, which could readily react with $\text{H}_2\text{O}/-\text{OH}$ or dissolved oxygen to be defluorinated. Thus, promoting the activation and conversion of terminal carboxyl ($-\text{CO}_2^-$) to $-\text{CO}_2\cdot$ could be beneficial for PFOA's degradation kinetics and defluorination efficiency.

Surface Frustrated Lewis pairs (SFLPs), Lewis acids and bases that are sterically prevented from the formation of Lewis acid-base adjuncts between organic molecules, recently have expanded to solid inorganic materials (Ma et al., 2018). It comprises adjacent Lewis acidic and

Lewis basic sites, which can provide synergetic activation sites to capture and react with stable small molecules (e.g., CO_2) under mild conditions (Stephan, 2016; Li et al., 2021). For example, Ozin et al. constructed SFLPs sites on $\text{In}_2\text{O}_{3-x}(\text{OH})_y$, with a coordinately unsaturated surface indium site (Lewis acid) proximal to an oxygen vacancy (O_v) and a surface hydroxide site (Lewis base), enabling the efficient conversion of CO_2 to CO or CH_3OH (Ghuman et al., 2016). Similarly, Yan's group created the SFLPs on $\text{CoGeO}_2(\text{OH})_2$ via a photogenerated holes oxidation process, showing an excellent capacity for CO_2 capture and reduction (Wang et al., 2018). The SFLPs promote the initial step of CO_2 photoreduction by accelerating the photoexcited electrons transfer from catalysts to CO_2 molecules, leading to the formation of bent $\text{CO}_2^{\cdot-}$ species (Fig. 1(a)) (Li et al., 2019). Hence, SFLPs catalysts show great potential in enhancing the activation and conversion of CO_2^- to $\text{CO}_2\cdot$ in the hole-dominated photocatalytic reaction (Fig. 1(b)), which is the initial and rate-limiting step for PFOA degradation (Eq. (2)).

$\text{Bi}_3\text{O}(\text{OH})(\text{PO}_4)_2$ (defined as BiOHP) is a photoexcited hole-dominated catalyst, and could be used for the photocatalytic degradation of PFOA (Sahu et al., 2018). Meanwhile, BiOHP is an oxyhydroxyphosphate salt with abundant terminal hydroxyls (Lewis bases) on the surfaces, which is a good candidate for constructing SFLPs (Li et al., 2021). Therefore, the engagement of SFLPs into BiOHP is of great promise to realize the effective activation of the terminal $-\text{CO}_2^-$ and efficient degradation of PFOA.

The construction of SFLPs is conducted via an *in-situ* light irradiation approach. Firstly, the BiOHP pre-catalyst was prepared by a versatile hydrothermal method (Sahu et al., 2018). The as-synthesized BiOHP pre-catalyst exhibits an octahedron morphology (Fig. S1). X-ray diffraction (XRD) pattern (Fig. 2(a)) confirms that the as-synthesized BiOHP pre-catalysts have a single pure crystalline phase, which can be ascribed to a typical

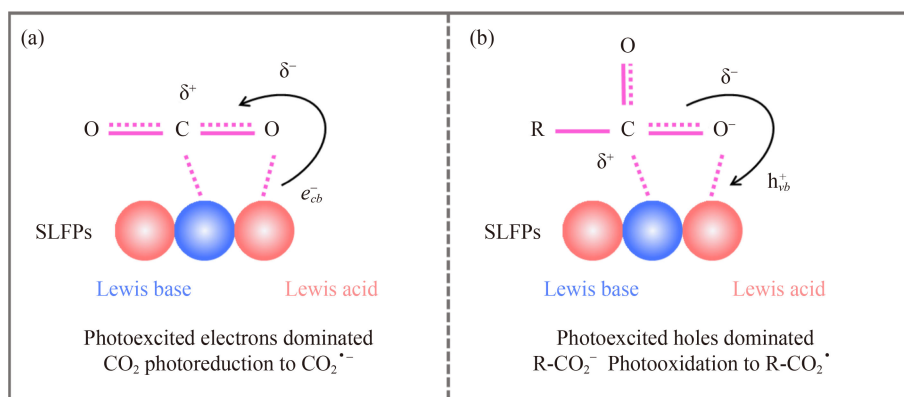


Fig. 1 (a) Schematic illustration for CO_2 photoreduction to $\text{CO}_2^{\cdot-}$ on SFLPs. (b) Proposed activation mechanism for R-CO_2^- photooxidation to $\text{R-CO}_2\cdot$.

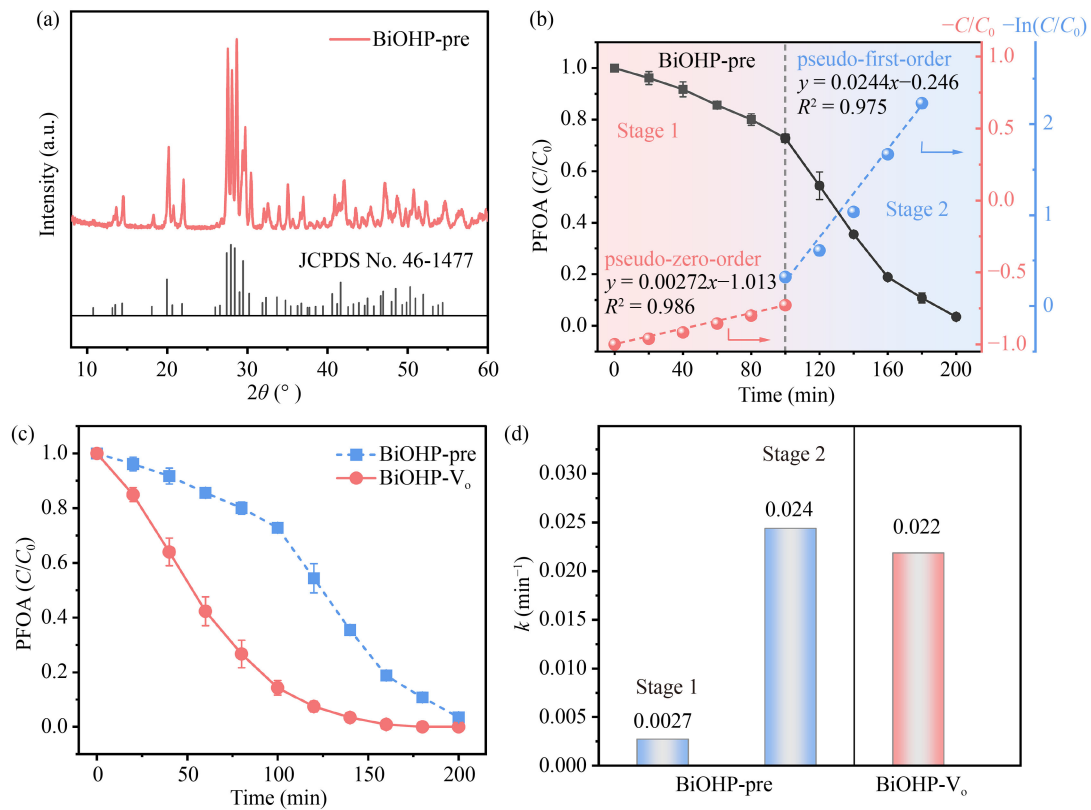


Fig. 2 (a) XRD pattern of the BiOHP pre-catalyst. (b) Time-dependent photodegradation of PFOA by the BiOHP pre-catalyst and corresponding kinetics fitting curves. (c) Comparison of degradation activity of the BiOHP pre-catalyst and BiOHP-V₀ toward PFOA and (d) corresponding kinetic constants.

Petitjeanite (JCPDS No. 46-1477). Interestingly, the BiOHP pre-catalyst exhibits two-stage photodegradation kinetics toward PFOA (Fig. 2(b)). Specifically, the degradation activity presents a pseudo-zero-order kinetic in the first stage, while it was fitted well with the pseudo-first-order kinetic model in the second stage. In addition, there is a significant difference in the rate constant between the two stages. The first stage shows a relatively slow rate constant (0.0027 min^{-1}), while the second stage's degradation kinetics was remarkably boosted by 9-fold. The distinct two-stage photodegradation process of PFOA might be attributed to the light-induced structural reconstruction on the BiOHP pre-catalysts.

To verify the light-induced reconstruction on BiOHP pre-catalysts, we treated the pre-catalysts by UV light irradiation for 2 h in deionized water, and the obtained product was defined as BiOHP-V₀. BiOHP-V₀ exhibits superior photocatalytic activity, with > 99% of PFOA degradation within 180 min (Fig. 2(c)). Intriguingly, BiOHP-V₀ only presents one-stage degradation kinetics, which is perfectly aligned with BiOHP pre-catalysts' rate constant in the second stage (Fig. 2(d)). Thus, UV light irradiation has triggered the microstructure reconstruction and optimization of BiOHP pre-catalysts. Correspondingly, photodegradation performance of BiOHP-V₀ toward PFOA was remarkably improved. Additionally, the color

of BiOHP-pre changed from white to light-grey after the UV irradiation (Fig. S2), with improvement in light-harvesting ability (Fig. S3). BiOHP-V₀ also exhibit higher adsorption capacity for PFOA than that of BiOHP-pre (Fig. S4), which is essential to the following photocatalytic oxidation process. Overall, the above merits of BiOHP-V₀ are conducive to promoting the photocatalytic degradation of PFOA.

The UV light irradiation may induce the generation of SFLPs on BiOHP, as the similar phenomenon was reported in oxyhydroxide photocatalysts (Wang et al., 2018). As a typical hole-dominant photocatalyst, the photogenerated holes of BiOHP could oxidize the lattice hydroxyls to produce O_v under light irradiation. Then, the coordinated unsaturated Bi sites proximity to O_v would be exposed and act as Lewis acid sites. Meanwhile, the adjacent hydroxyls could behave as Lewis base, resulting in the fabrication of Lewis acid-base proximal sites and the formation of SFLPs (Fig. S5).

To further account for the contribution of SFLPs to photocatalytic performance, we attempt to tune the concentration of O_v and surface hydroxyls, which are the essential components of SFLPs, by a calcination process (Hoch et al., 2016). According to the thermogravimetry (TG) and differential scanning calorimetry (DSC) analysis (Fig. S6), the weight of the BiOHP-V₀ slightly

improves with the annealing treatment, due to the partial oxidation of BiOHP to Bi_2O_3 at high temperature. A remarkable endothermic peak starting from 405 °C and ending at 645 °C is clearly observed, which may be associated with the structural transformation. Therefore, two temperatures (380 °C and 280 °C) lower than the structural transformation turning point (405 °C), are adopted as calcination temperatures, which would tune the concentration of O_v and surface hydroxyls without changing BiOHP structural composition. Both BiOHP-280 and BiOHP-380 exhibit similar XRD diffraction peaks to BiOHP- V_o (Fig. S7), indicating good structural

stability with low calcination temperature treatment. Additionally, the micro-morphology of the BiOHP-280 and BiOHP-380 were also aligned with BiOHP- V_o (Fig. S8).

Distinctive peaks located at $g = 2.003$ are observed in the electron paramagnetic resonance (ERP) spectra for all the BiOHP samples (Fig. 3(a)), confirming the existence of O_v . Notably, the highest concentration of O_v is found in BiOHP- V_o , which gradually decreases with the increase of calcination temperature. X-ray photoelectron spectroscopy (XPS) analysis demonstrated that the peaks of Bi 4f shifted to higher binding energy, from 164.77 to 164.90 and 165.03 eV, which can be attributed to the

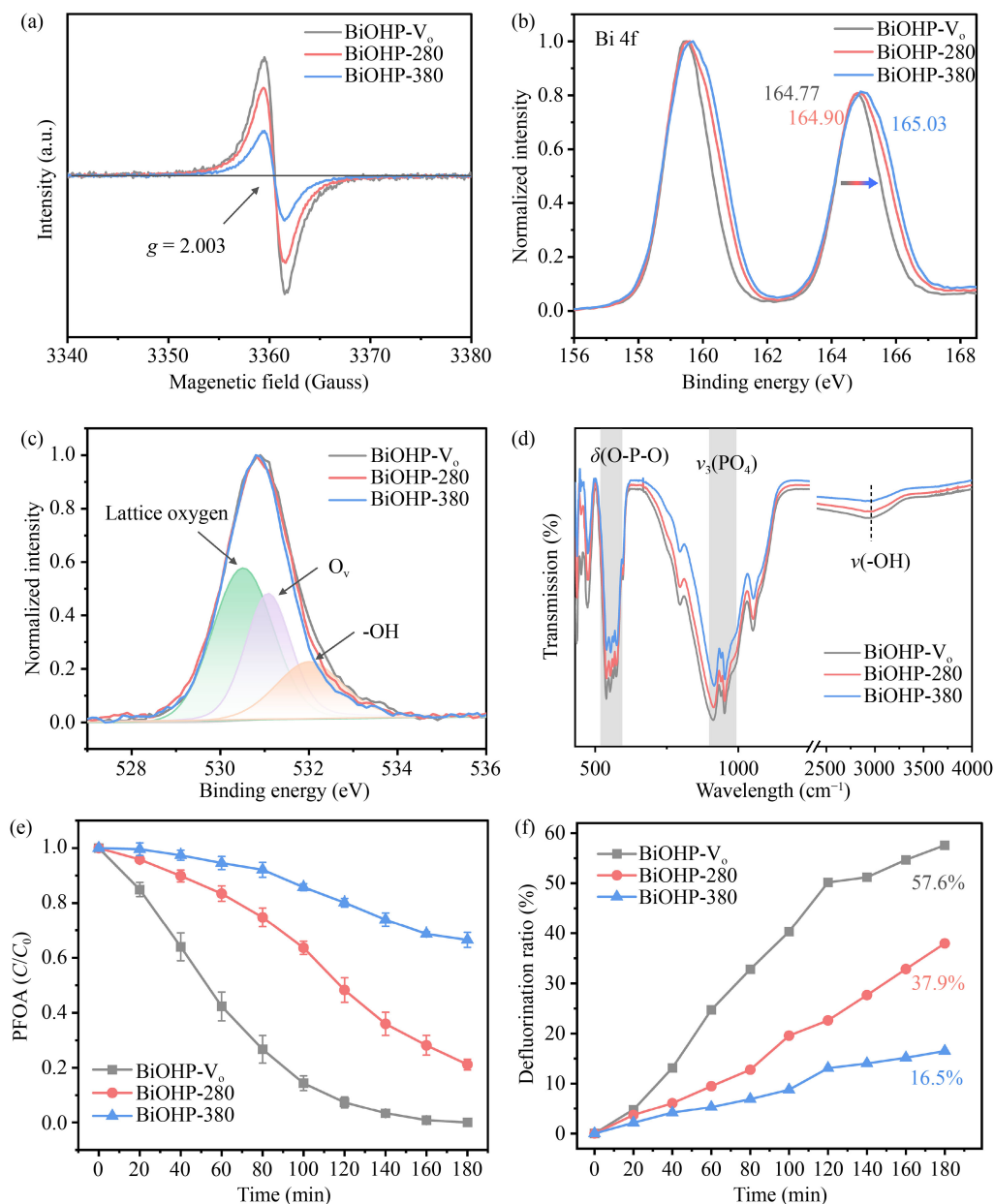


Fig. 3 (a) EPR analysis of BiOHP- V_o , BiOHP-280 and BiOHP-380 at 77K. (b) Bi 4f and (c) O 1s XPS spectra and (d) ATR-FTIR spectra of the BiOHP- V_o , BiOHP-280 and BiOHP-380. (e) Comparison of the degradation performance and (f) corresponding defluorination efficiency over the BiOHP- V_o , BiOHP-280 and BiOHP-380 photocatalysts.

formation of the coordinated unsaturated Bi-metal sites adjacent to O_v (Fig. 3(b)). The O 1s XPS spectra can be deconvoluted into three distinct peaks (Fig. 3(c)), ascribing to the lattice oxygen (530.5 eV), O_v (531.1 eV) and hydroxides (532.0 eV) (Hoch et al., 2016). Notably, it shows that the peaks ascribed to O_v and hydroxides gradually reduced with improving the calcination temperature, indicating the O_v and surface hydroxyl decreased during the calcination process. On the other hand, the -OH stretches' intensity in the Fourier transform infrared spectroscopy (FTIR) spectra decreases with increasing calcination temperature (Fig. 3(d)), illustrating that samples treated at higher temperatures have lower hydroxide contents. Taking the above investigation together, BiOHP- V_o presents the highest content in both O_v (associated with the formation of Lewis acidic Bi sites) and the surface hydroxide (Lewis base). Thus, BiOHP- V_o exhibits the highest SFLPs concentration, and the increase of calcination temperature would lower the concentration of SFLPs.

Not surprisingly, the degradation activity of BiOHP-280 and BiOHP-380 drops sharply compared to BiOHP- V_o (Fig. 3(e)), which is highly correlated with the concentration of SFLPs. While neglectable difference is found in specific surface area of all BiOHP samples (Table S1), indicating a minimum effect of surface area on the degradation activity. Thus, the SFLPs concentration is the dominant contributor on the PFOA's photocatalytic degradation. Additionally, the BiOHP- V_o exhibits superior defluorination ability for PFOA, achieving a defluorination efficiency of 57.6% within 180 min (Fig. 3(f)), which is much higher than most previously reported photocatalysts (Table S2). The generated reactive oxygen species (Fig. S9) and intermediates during the degradation process were also analyzed to reveal the degradation pathways. The degradation of PFOA by BiOHP- V_o photocatalysts experiences a stepwise photooxidation process (Fig. S10).

Based on the abovementioned results, we proposed a mechanism for photocatalytic degradation of PFOA over the BiOHP- V_o photocatalyst (Fig. S11(a)). The most critical process for PFOA degradation is to activate the terminal $-CO_2^-$, which is a rate-limiting step (Eq. (2)). Under UV light irradiation, the photogenerated holes could oxidize the lattice hydroxyls to generate O_v . Then, SFLPs were formed due to the exposure of coordinated unsaturated Bi sites (Lewis acid) in proximity to O_v and their adjacent hydroxyls (Lewis base) (step 1 in Fig. S11(a)). The SFLPs promote the $-CO_2^-$ adsorption on the catalyst surface, as the carbon in the terminal $-CO_2^-$ of PFOA tends to be captured by the Lewis basic -OH, while the oxygen was absorbed on the Lewis acidic Bi sites (step 2 in Fig. S11(a)). Afterwards, the photoexcited holes induced the rapid charge transfer from the $-CO_2^-$ to BiOHP- V_o , leading to the release of $R-CO_2\cdot$ (step 3 in Fig. S11(a)). Particularly, O_v and surface hydroxyl groups

could create mid-gap states that act as shallow donors and acceptors, respectively (Fig. S11(b)). The multiply charge transfer pathways provide an accessible way for photogenerated carriers' transport and separation. Furthermore, the existence of these mid-gap states prolongs the lifetime of the photogenerated carriers, which is also beneficial for enhancing photocatalytic activity (He et al., 2016).

In summary, a UV-light-induced strategy was employed to construct SFLPs over BiOHP photocatalysts. The SFLPs consist of Lewis acidic coordinately unsaturated surface bismuth sites that associated with the produced O_v during light irradiation and their adjacent Lewis basic -OH. The SFLPs-abundant BiOHP shows high catalytic activity in photodegradation of PFOA, benefiting from their rapid activation of the terminal $-CO_2^-$, which is a rate-limiting step for PFOA decomposition. Consequently, we provide novel insights into the activation and degradation of PFOA by SFLPs, shedding light on photocatalytic decontaminant for persistent organic pollutants.

Acknowledgements This research was financially supported by the National Natural Science Foundation of China (Nos. 22006088 and 42077293), the Natural Science Foundation of Guangdong Province (China) (No. 2019QN01L797), the Shenzhen Municipal Science and Technology Innovation Committee (China) (Nos. WZC20200817103 015002 and RCYX20210609104448111), and the Tsinghua Shenzhen International Graduate School (China) (Nos. HW2020002 and QD2021010N).

Electronic Supplementary Material Supplementary material is available in the online version of this article at <https://doi.org/10.1007/s11783-023-1603-6> and is accessible for authorized users.

References

- Cordner A, Goldenman G, Birnbaum L S, Brown P, Miller M F, Mueller R, Patton S, Salvatore D H, Trasande L (2021). The true cost of PFAS and the benefits of acting now. *Environmental Science & Technology*, 55(14): 9630–9633
- Ding W, Tan X, Chen G, Xu J, Yu K, Huang Y (2021). Molecular-level insights on the facet-dependent degradation of perfluorooctanoic acid. *ACS Applied Materials & Interfaces*, 13(35): 41584–41592
- Garnett J, Halsall C, Thomas M, Crabeck O, France J, Joeris H, Ebinghaus R, Kaiser J, Leeson A, Wynn P M (2021). Investigating the uptake and fate of poly- and perfluoroalkylated substances (PFAS) in sea ice using an experimental sea ice chamber. *Environmental Science & Technology*, 55(14): 9601–9608
- Ghuman K K, Hoch L B, Szymanski P, Loh J Y Y, Kherani N P, El-Sayed M A, Ozin G A, Singh C V (2016). Photoexcited surface frustrated Lewis pairs for heterogeneous photocatalytic CO_2 reduction. *Journal of the American Chemical Society*, 138(4): 1206–1214
- He L, Wood T E, Wu B, Dong Y, Hoch L B, Reyes L M, Wang D, Kübel C, Qian C, Jia J, Liao K, O'Brien P G, Sandhel A, Loh J Y

- Y, Szymanski P, Kherani N P, Sum T C, Mims C A, Ozin G A (2016). Spatial separation of charge carriers in $\text{In}_2\text{O}_{3-x}(\text{OH})_y$ nanocrystal superstructures for enhanced gas-phase photocatalytic activity. *ACS Nano*, 10(5): 5578–5586
- Hoch L B, Szymanski P, Ghuman K K, He L, Liao K, Qiao Q, Reyes L M, Zhu Y, El-Sayed M A, Singh C V, Ozin G A (2016). Carrier dynamics and the role of surface defects: designing a photocatalyst for gas-phase CO_2 reduction. *Proceedings of the National Academy of Sciences of the United States of America*, 113(50): E8011–E8020
- Li T, Zhang W, Qin H, Lu L, Yan S, Zou Z (2021). Inorganic frustrated Lewis pairs in photocatalytic CO_2 reduction. *ChemPhotoChem*, 5(6): 495–501
- Li X, Yu J, Jaroniec M, Chen X (2019). Cocatalysts for selective photoreduction of CO_2 into solar fuels. *Chemical Reviews*, 119(6): 3962–4179
- Li X, Zhang P, Jin L, Shao T, Li Z, Cao J (2012). Efficient photocatalytic decomposition of perfluorooctanoic acid by indium oxide and its mechanism. *Environmental Science & Technology*, 46(10): 5528–5534
- Liu X, Wei W, Xu J, Wang D, Song L, Ni B J (2020). Photochemical decomposition of perfluorochemicals in contaminated water. *Water Research*, 186: 116311
- Lu D, Sha S, Luo J, Huang Z, Jackie X Z (2020). Treatment train approaches for the remediation of per- and polyfluoroalkyl substances (PFAS): a critical review. *Journal of Hazardous Materials*, 386: 121963
- Ma Y, Zhang S, Chang C R, Huang Z Q, Ho J C, Qu Y (2018). Semi-solid and solid frustrated Lewis pair catalysts. *Chemical Society Reviews*, 47(15): 5541–5553
- Mumtaz M, Bao Y, Li W, Kong L, Huang J, Yu G (2019). Screening of textile finishing agents available on the Chinese market: an important source of per- and polyfluoroalkyl substances to the environment. *Frontiers of Environmental Science & Engineering*, 13(5): 67
- Ng C, Cousins I T, DeWitt J C, Glüge J, Goldenman G, Herzke D, Lohmann R, Miller M, Patton S, Scheringer M, Trier X, Wang Z (2021). Addressing urgent questions for PFAS in the 21st century. *Environmental Science & Technology*, 55(19): 12755–12765
- Qian Y, Qiao W, Zhang Y (2021). Toxic effect of sodium perfluorononyloxy-benzenesulfonate on *Pseudomonas stutzeri* in aerobic denitrification, cell structure and gene expression. *Frontiers of Environmental Science & Engineering*, 15(5): 100
- Qiao W, Li R, Tang T, Zuh A A (2021). Removal, distribution and plant uptake of perfluorooctane sulfonate (PFOS) in a simulated constructed wetland system. *Frontiers of Environmental Science & Engineering*, 15(2): 20
- Sahu S P, Qanbarzadeh M, Ateia M, Torkzadeh H, Maroli A S, Cates E L (2018). Rapid degradation and mineralization of perfluorooctanoic acid by a new petitjeanite $\text{Bi}_3\text{O}(\text{OH})(\text{PO}_4)_2$ microparticle ultraviolet photocatalyst. *Environmental Science & Technology Letters*, 5(8): 533–538
- Stephan D W (2016). The broadening reach of frustrated Lewis pair chemistry. *Science*, 354(6317): aaf7229
- Sun Q, Zhao C, Frankcombe T J, Liu H, Liu Y (2020). Heterogeneous photocatalytic decomposition of per- and poly-fluoroalkyl substances: a review. *Critical Reviews in Environmental Science and Technology*, 50(5): 523–547
- Tan X, Chen G, Xing D, Ding W, Liu H, Li T, Huang Y (2020). Indium-modified Ga_2O_3 hierarchical nanosheets as efficient photocatalysts for the degradation of perfluorooctanoic acid. *Environmental Science. Nano*, 7(8): 2229–2239
- Wang X, Lu L, Wang B, Xu Z, Xin Z, Yan S, Geng Z, Zou Z (2018). Frustrated Lewis pairs accelerating CO_2 reduction on oxyhydroxide photocatalysts with surface lattice hydroxyls as a solid-state proton donor. *Advanced Functional Materials*, 28(43): 1804191
- Yang Y (2020). Recent advances in the electrochemical oxidation water treatment: spotlight on byproduct control. *Frontiers of Environmental Science & Engineering*, 14(5): 85
- Zheng G, Schreder E, Dempsey J C, Uding N, Chu V, Andres G, Sathyanarayana S, Salamova A (2021). Per- and polyfluoroalkyl substances (PFAS) in breast milk: concerning trends for current-use PFAS. *Environmental Science & Technology*, 55(11): 7510–7520